Liquid Crystals
Publication details, including instructions for authors and subscription information:
http://www.informaworld.com/smpp/title~content=t713926090

Characterization of a new chiral antiferroelectric liquid crystal with a lateral bromo substituent

P. Gisse; P. Cluzeau; V. Ravaine; H. T. Nguyen

Online publication date: 11 November 2010

To cite this Article Gisse, P. , Cluzeau, P. , Ravaine, V. and Nguyen, H. T.(2002) 'Characterization of a new chiral antiferroelectric liquid crystal with a lateral bromo substituent', Liquid Crystals, 29: 1, 91 — 98
To link to this Article: DOI: 10.1080/02678290110093813
URL: http://dx.doi.org/10.1080/02678290110093813

LIQUID CRYSTALS, 2002, VOL. 29, NO. 1, 91–98

Characterization of a new chiral antiferroelectric liquid crystal with a lateral bromo substituent

P. GISSE*
Laboratoire de Physique de la Matière Condensée, 33 rue St Leu, 80039 Amiens, France

P. CLUZEAU
Laboratoire de Dynamique et Structure des Matériaux Moléculaires, Université de Lille 1, 59655 Villeneuve d'Ascq, Cedex, France

V. RAVAINE
ENSCPB, LACReM, Université de Bordeaux 1, 33405 Talence, France

and H. T. NGUYEN
Centre de Recherche Paul Pascal, CNRS, Av Schweitzer, 33600 Pessac, France

(*Received 14 May 2001; in final form 7 July 2001; accepted 12 July 2001*)

In this paper we present the characterization of a new chiral mesogen with a lateral bromo substituent. The identification of the various smectic phases is achieved by texture observation, miscibility studies and DSC. The optic and electro-optic properties are also investigated. The real part of the complex dielectric permittivity as a function of the temperature was also measured in the planar geometry for thin samples. The dielectric behaviour will be qualitatively discussed on the simple assumption of different anchorings. These results point out the importance of anchoring conditions in relation to the macroscopic properties observed in very thin cells of antiferroelectric liquid crystals.

1. Introduction

Since the discovery of the ferroelectric phase (SmC*), several smectic variants distinguished by their behaviour under electric fields have been identified. Some of them are of technological interest [1, 2], for example, the antiferroelectric (SmC^*_A) phase. The others are of rather intellectual interest, like the ferrielectric (SmC^*_{FI}) phases. In any case, since the identification of the smectic C* variants of MHPOBC, some properties of these phases remain subject to controversy, as for instance the exact structure of the SmC^*_{FI} phases. The successful application of the resonant scattering technique at the sulphur K edge has clarified the situation and shown the existence of two-, three- and four-layer periodicities, respectively, in the SmC^*_A SmC^*_{FI1}, and SmC^*_{FI2} phases [3, 4]. Nevertheless, some discrepancies remain between the resonant X-ray scattering results and optical measurements [4]; that is the reason why new scattering experiments on materials containing other resonant atoms are expected.

In this paper we present the characterization of a new chiral molecule with a lateral bromo substituent, specially designed for resonant X-ray diffraction. The results of the resonant X-ray diffraction obtained on this compound have already been reported in a separate publication [5]. Here, the various phases are studied by texture observation, miscibility experiments and DSC. The optic and electro-optic properties are also investigated, as well as the dielectric behaviour of the different smectic phases measured in the planar geometry for thin samples.

2. Material and mesomorphic properties

The compound studied in this paper is prepared following the scheme:

*Author for correspondence;
e-mail: patrick.gisse@sc.u-picardie.fr

Liquid Crystals ISSN 0267-8292 print/ISSN 1366-5855 online © 2002 Taylor & Francis Ltd
http://www.tandf.co.uk/journals
DOI: 10.1080/02678290110093813

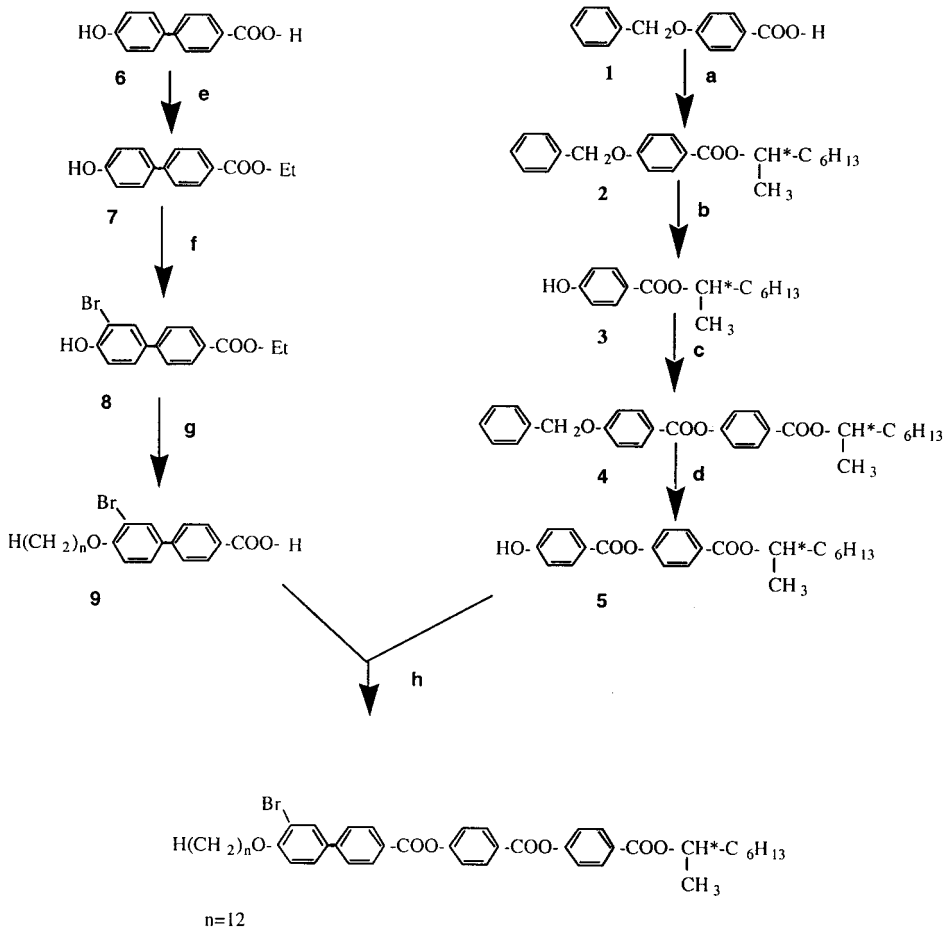

(a) DCC, DMPA, CH_2Cl_2, (*R*)-2-octanol
(b) H_2, Pd/C, EtAcO
(c) DCC, DMAP, CH_2Cl_2, $PhCH_2O-Ph-COOH$
(d) H_2, Pd/C, EtAcO
(e) EtOH, H_2SO_4 reflux
(f) Br_2, $CHCl_3$
(g) $H(CH_2)n$-Br, KOH, EtOH
(h) DCC, DMAP, CH_2Cl_2

Scheme.

The final compound is obtained by an esterification reaction between the (*R*)-phenol (**5** in the above scheme) [6] and 3-bromo-4-dodecyloxybiphenyl-4′-carboxylic acid (**9** in the above scheme) in dichloromethane in the presence of DCC and DMAP. It was purified by chromatography over silica gel with dichloromethane as eluent. The pure product was crystallized from absolute ethanol. Its mesomorphic sequence is:

Cr 75.1 SmC^*_A 109.5 SmC^*_{FI} 110 SmC* 175 SmA 195 I (°C).

Temperatures were recorded in DSC scans on heating at 3 K min^{-1}. On cooling from the isotropic liquid, the SmA phase is obtained with the focal-conic optical texture and (or) the homeotropic texture. On further cooling, the SmC* phase appears with striated focal-conics and the homeotropic domains become coloured. Cooling the SmC* phase to the SmC^*_{FI} and then the SmC^*_A phase induces a rapid motion in the homeotropic domains characteristic of the ferrielectric phase. The temperature range of this single SmC^*_{FI} phase is very narrow. Miscibility of the new compound with the $n=10$ homologue of the well known thiobenzoate *n*OTBBB1M7 series was investigated in order to identify the observed mesophases. The bulk C_{10} thiobenzoate shows the following phase sequence:

Cr 106 SmC^*_A 112 SmC^*_{FI1} 114 SmC^*_{FI2} 119.2 SmC* 120 SmC^*_α 122 SmA 150 I (°C)

This material exhibits two ferrielectric phases [7], but the SmC^*_{FI1}–SmC^*_{FI2} transition could not be traced for all compositions of the binary mixtures. Consequently, the nature of the ferrielectric phase of the brominated compound could not be inferred from this miscibility study. On the other hand, the SmC^*_A, SmC* and SmA phases are individually continuously connected and therefore unambiguously identified.

3. Optic and electro-optic experiments

Helical pitch measurements were performed both by the Grandjean–Cano (GC) method and by analysing the selectively reflected light. The samples were heated using a Mettler FP5 hot stage (accuracy 0.1°C). The appropriate alignment for the SmC* (or SmC^*_A) phase in the prismatic sample is pseudo-homeotropic [8]. In such an orientation the smectics layers are roughly parallel to the substrate and the angular position of the molecules on the smectic cone is set by the rubbing on the glass plates. Moreover the analysis of the light selectively reflected by flat pseudo-homeotropic drops laid on a glass slide coated with silane provides accurate pitch values, especially for the SmC^*_A phase where a small number of GC steps are obtained. The spectral analysis was performed using a 270M-Jobin–Yvon spectrometer [9].

In order to study the electro-optic properties, the material was confined between two ITO coated glass slides separated by 7.5 μm thick spacers, with an active electrode surface of 25 mm^2. The homogeneous planar geometry was obtained by using a rubbed polyimide alignment layer. It was improved both by using slow cooling (0.1°C min^{-1}) through the isotropic to SmA phase transition, and also by applying an a.c. electric field of 0.2 V μm^{-1} at a frequency of 20 Hz in the vicinity of the SmC–SmC* phase transition on cooling. The quality of the alignment was checked by polarizing optical microscopy. The variation of the spontaneous polarization with temperature was examined under the same electric field conditions, namely saturated conditions [10], by detecting the switching current under a triangular wave electric field. The apparent tilt angle was measured as a function of temperature, using the well known 'switching' method [11]. This method consists in unwinding the helicoidal structures by applying a sufficiently strong square wave electric field of low frequency (10 V μm^{-1} at a frequency of 0.2 Hz) to the complex, dipolar, ordered smectic phases, and measuring the angular difference between two extinction positions through crossed polarizers.

The conventional dielectric measurements [12, 13] in the frequency range from 10 Hz to 1 MHz were made using an impedance analyser (Schlumberger 1260).

4. Results and discussion

Let us first analyse the helical pitch behaviour through the different smectic phases (figure 1). The pitch in the SmC^*_A phase is almost constant: it varies on heating from -0.32 μm at lower temperatures to -0.43 μm just below the ferrielectric phase transition. This is also the case in the SmC* phase within which the helix pitch is about $+0.65$ μm. The minus and plus signs for the pitch values, respectively, in the SmC^*_A and SmC* phases only indicate that the sense of rotation of the twist is inverted. It can often be associated with a reversal of the sense of the helix [14] which occurs in the ferrielectric phase. In the SmC^*_A phase the selective reflection of the light always corresponds to $\lambda = np$ (where λ is the reflected wavelength, n the average refractive index ($n = 1.5$) and p the pitch value); as for the SmC* phase the selective reflection corresponds to $\lambda = np$ or to $\lambda = 2np$ for pitch values smaller than 0.3 μm (this limit of 0.3 μm is fixed by the sensitivity of the spectrometer). The pitch measurement on cooling is given only to show the existence of the hysteresis on crossing through the SmC^*_A–SmC^*_{FI}–SmC* phases transitions. This hysteresis is large considering that in the homeotropic geometry the molecular anchoring energy is weak.

Figure 2 shows the variation of the spontaneous polarization versus temperature, $\mathbf{P}_s(T)$. The frequency of the triangular wave is 54 Hz, and the maximum field value is 10 V μm^{-1}. This field is high enough to switch the ferrielectric and antiferroelectric phases into the homogeneous ferroelectric phase. Under these conditions, no anomaly could be detected on the $\mathbf{P}_s(T)$ curve at the phase transitions. The value of the saturated polarization close to the ferroelectric–antiferroelectric phase transition is around 90 nC cm^{-2}.

The variation in the tilt angle as a function of temperature shows no anomaly at the smectic phase transitions except to T_c, where a tail due to the classical electroclinic effect is always observed. The saturated value of the apparent tilt angle is around 32° within an accuracy of 1°, which seems to be consistent with the value of the steric angle obtained from X-ray measurements [15].

We have also measured the complex dielectric constant as a function of temperature for various frequencies. Note that for each temperature, the value of the real $\varepsilon'(w)$ and imaginary $\varepsilon''(w)$ parts of the dielectric constant $\varepsilon^*(w)$ were corrected taking into account the resistivity of the ITO plates and the conductivity of the material extrapolated to zero frequency.

In figure 4, we present the variation of the real part of the permittivity for several frequencies as a function of temperature as recorded during: (*a*) the cooling and (*b*) the heating process. The cooling (heating) rate is now 0.1°C min^{-1}. This dielectric measurement does not allow us to distinguish easily the different smectic phases

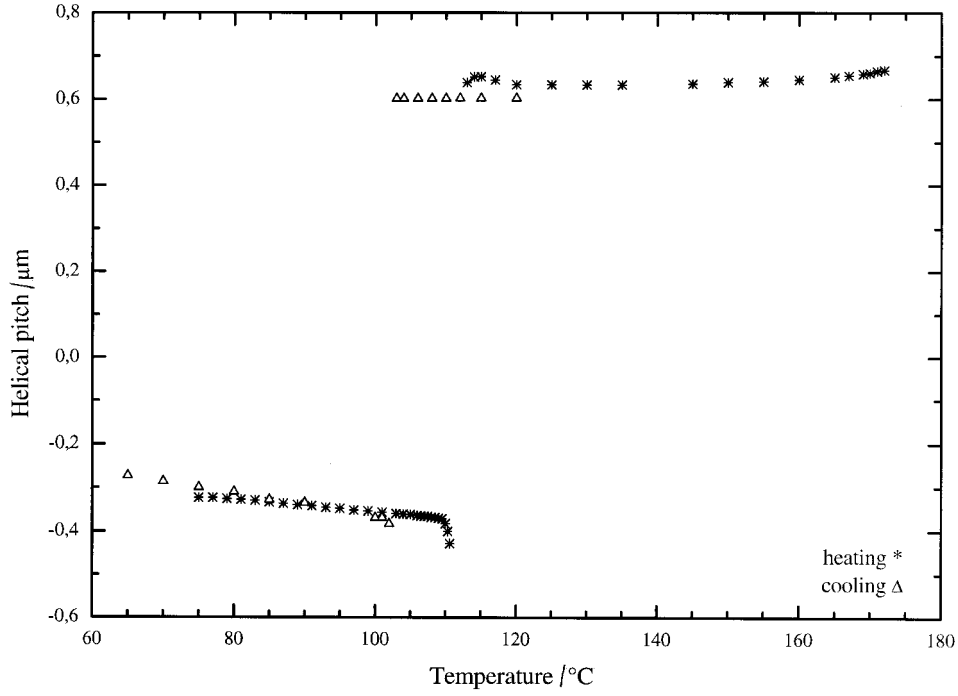

Figure 1. Helical pitch versus temperature on heating and on cooling (respectively, star and open triangle).

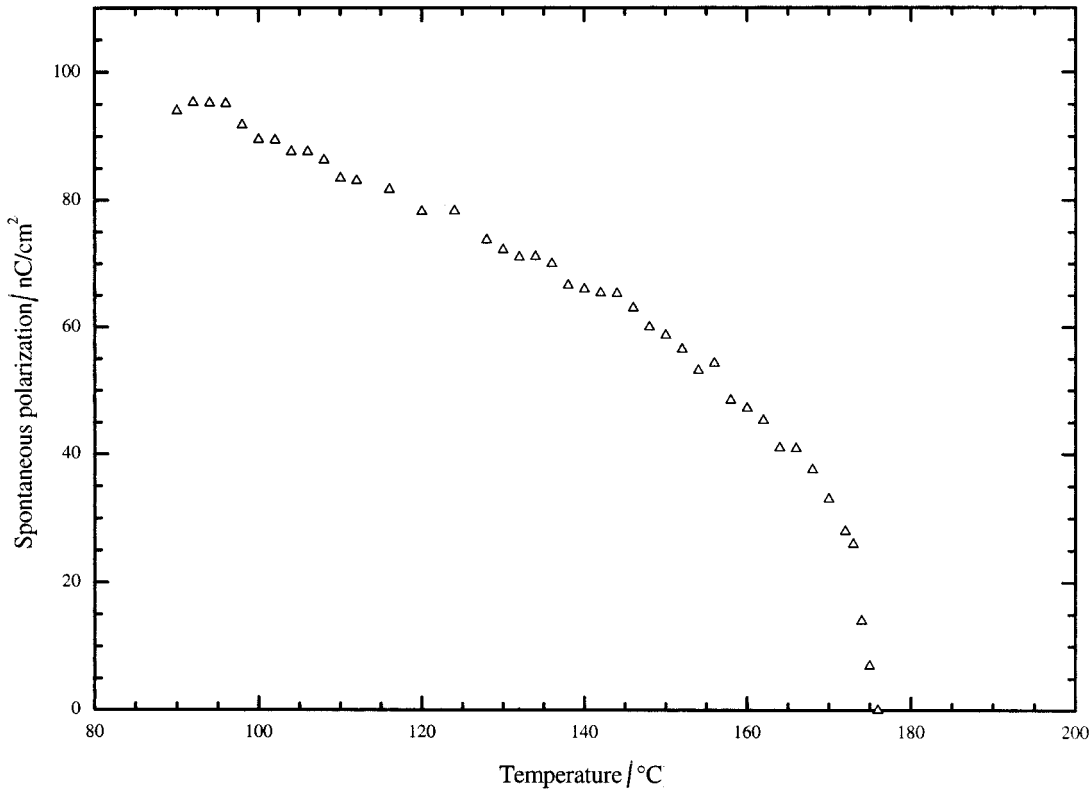

Figure 2. Temperature dependence of the spontaneous polarization under a triangular wave electric field and saturated conditions, in a 7.5 µm planar cell.

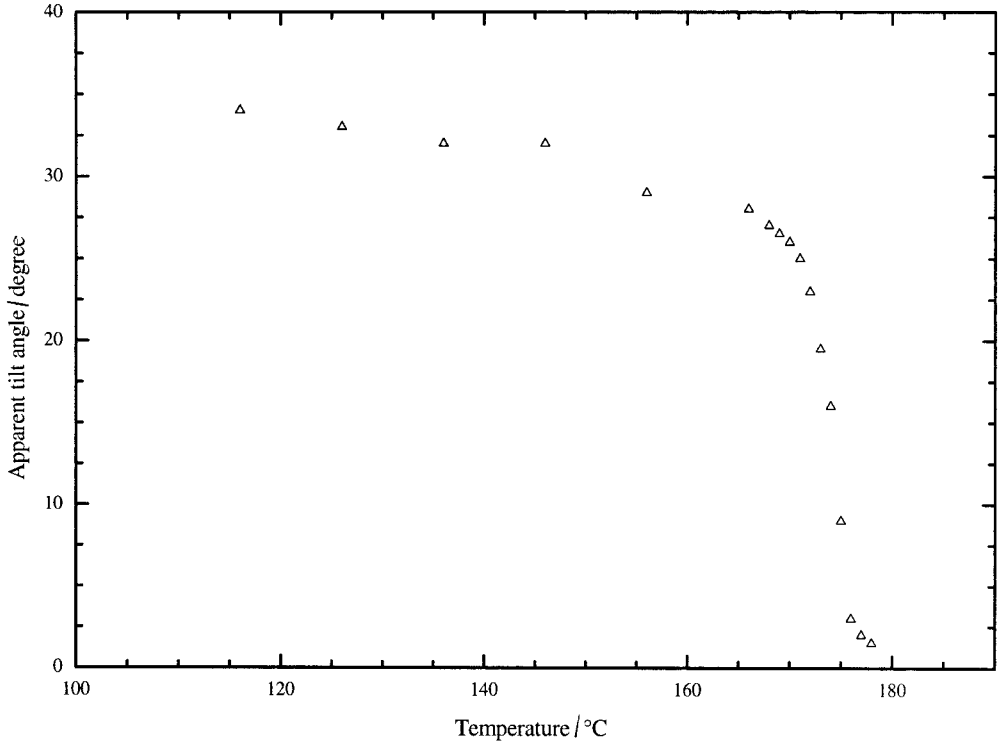

Figure 3. Temperature dependence of the apparent tilt angle under a square wave electric field of low frequency in saturated conditions, in a 7.5 μm planar cell.

and the transition temperatures between them, except for the SmA–SmC* transition. However, we note that the real part of the complex permittivity for 1 kHz in the SmA phase is small and quite constant. It exhibits a drastic increase in the vicinity of the transition (close to $T = 176.8$°C) from the SmA to the SmC* phase due to the appearance of the ferroelectric helical structure. This transition temperature between the paraelectric and the ferroelectric phase can be reported as the maximum in the real part of the complex permittivity at low frequency and the minimum for high frequency according to [16]. The associated Goldstone mode relaxation gives the most important contribution in ε' at this frequency. The relaxation frequency of this mode was measured as nearly 3 kHz, almost temperature independent in the ferroelectric phase as already published [17]. Obviously during the cooling process, we can observe a smooth increase in the value of the real part of the complex permittivity for low frequencies, inside the ferroelectric phase close to 120°C.

The last remark we make on comparing figures 4(*a*) and 4(*b*), concerns the important spread in the transition temperature in the vicinity of the SmC_A^* phase, 4(*a*), compared with the DSC results (109.5°C). In fact, the SmC_A^* phase is well characterized in dielectrics by a very weak value in ε' independent of the frequency, as observed below 75°C, in our cell of 7.5 μm thickness, during the cooling process. Let us focus on this last point in relation to figure 5. The behaviour of the real part of the complex permittivity for 1 kHz is reported on heating as well as on cooling, at a rate of 0.1°C min^{-1} in the SmC_A^*–SmC_{FI}^*–SmC* temperature range. We can note that during the heating process the amplitude of the real part of the permittivity remains weak close to $T = 115$°C which suggests that the antiferroelectric character remains in this temperature range. Such thermal hysteresis seen in ε' has already been mentioned in the range of the antiferroelectric phase for other compounds [18]. The same important conclusion can be reached in our case, in relation to the decreasing amplitude of this thermal hysteresis for thicker cells.

We can qualitatively explain the behaviour of ε' in the antiferroelectric phase, taking into account the surface anchoring energy already described in [19]. In a first approximation (when the surface anchoring state is assumed independent of the bulk), this anchoring energy can be written in a general form as a function of two polarization (**P**) and antipolarization (**A**) vectors. $\mathbf{P}_0$ is the magnitude of the spontaneous polarization and γ_1, γ_2, γ_3 are the anchoring constants.

$$W = -\gamma_1(\mathbf{n}\ \mathbf{P}/\mathbf{P}_0)^2 - \gamma_2(\mathbf{n}\ \mathbf{P}) - \gamma_3(\mathbf{n}\ \mathbf{A})^2$$

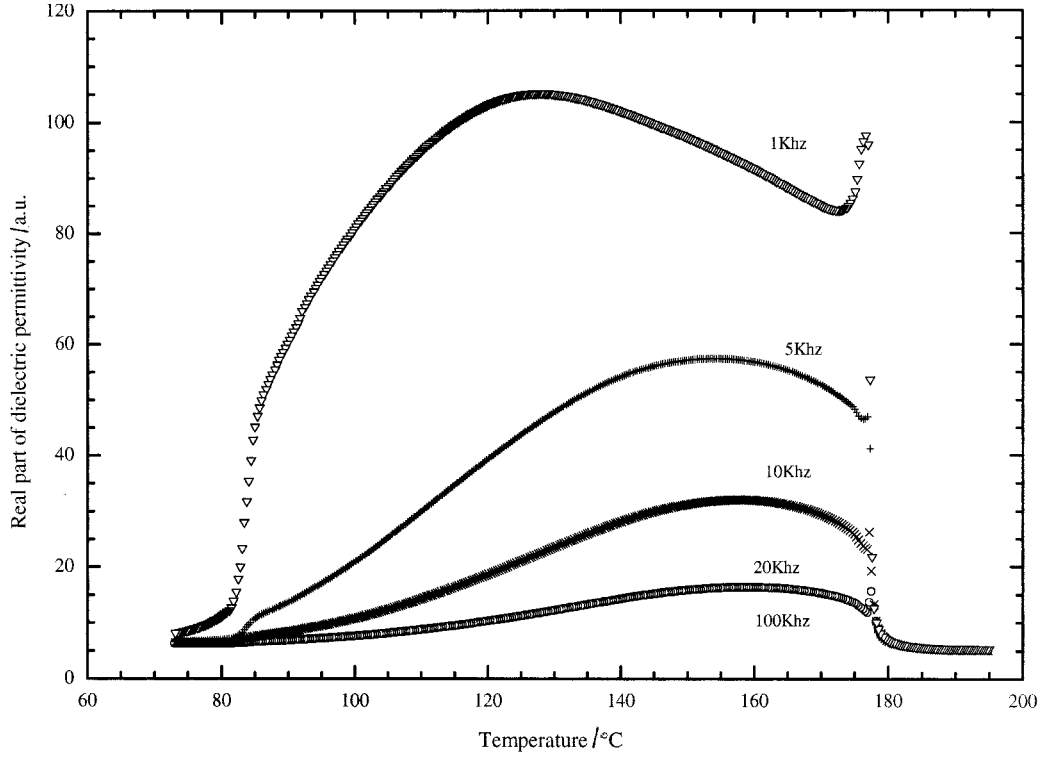

(*a*)

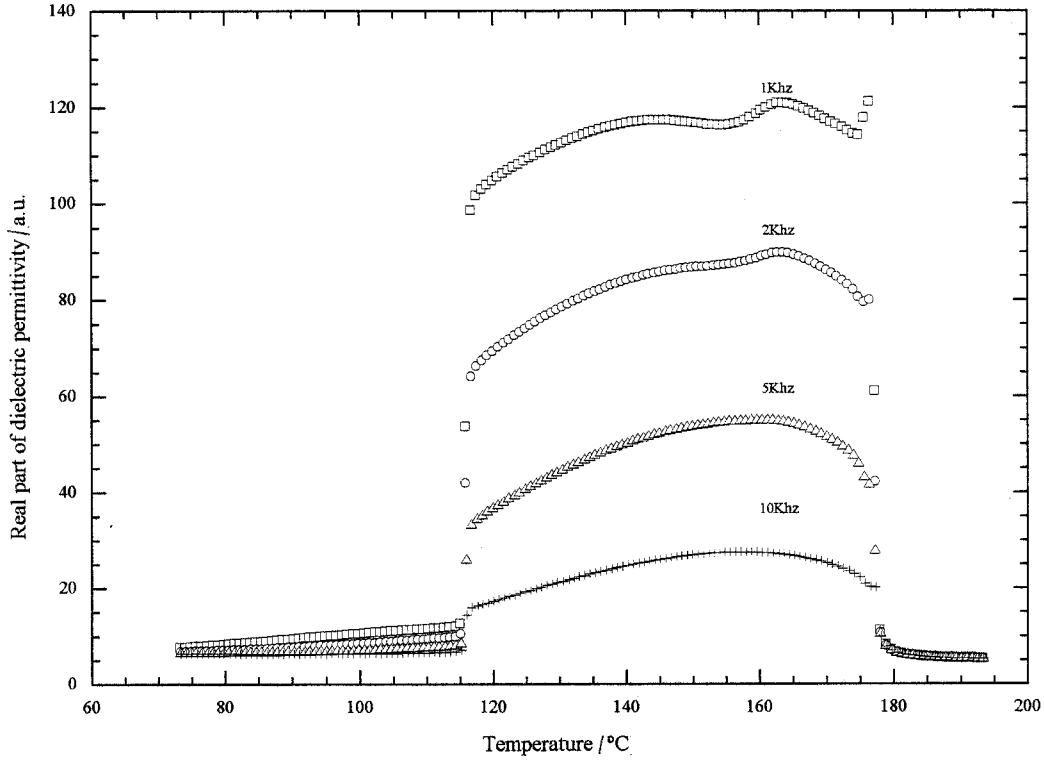

(*b*)

Figure 4. (*a*) Real part of the complex dielectric permittivity versus temperature, during a cooling process (rate 0.1°C min^{-1}), for the following frequencies: 1, 5, 10, 20, 100 kHz. (*b*) Real part of the complex dielectric permittivity versus temperature, during a heating process (rate 0.1°C min^{-1}), for the following frequencies: 1, 2, 5, 10 kHz.

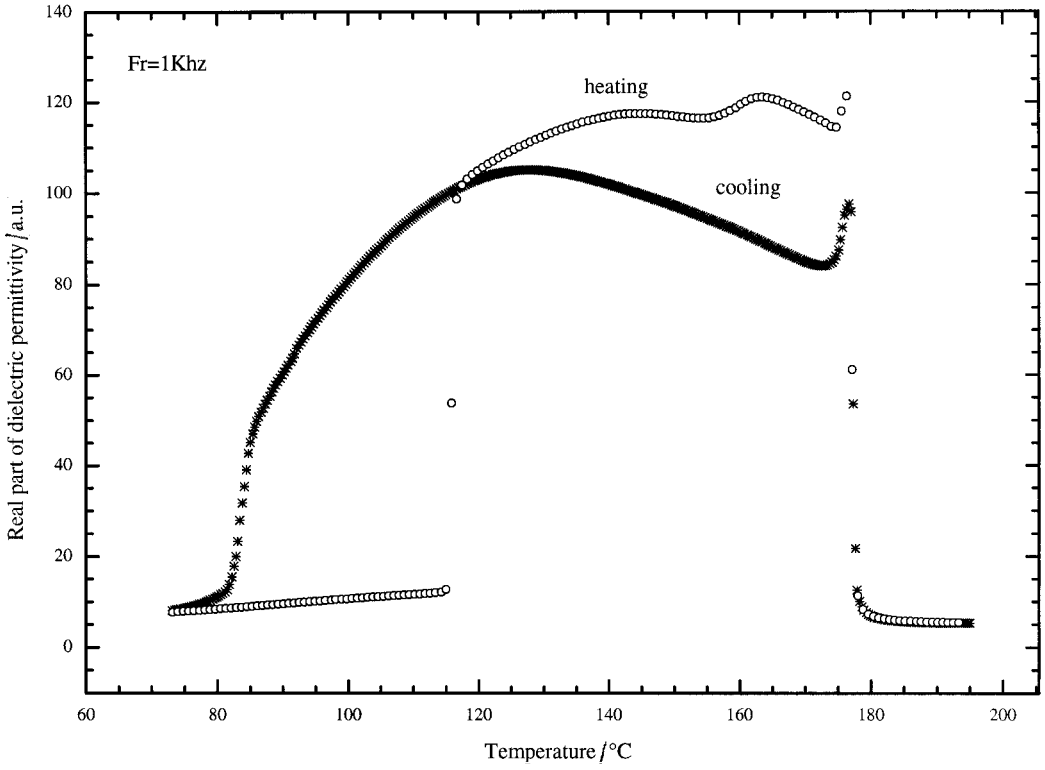

Figure 5. Real part of the complex dielectric permittivity versus temperature during both cooling and heating processes for 1 kHz.

which can be rewritten as

$$W(\phi, \psi) = -\cos^2\phi\cos^2\psi - \gamma_F\cos\phi\cos\psi - \gamma_{AF}\sin^2\phi\sin^2\psi$$

with $\phi = (\phi_i + \phi_{i+1})/2$ and $\psi = (\phi_i - \phi_{i+1})/2$, where ϕ_i is the azimuthal angle in the ith layer and γ_F, γ_{AF} are the recalculated anchoring coefficients. One can also expect three possible anchorings exhibiting three local or absolute minima, when the influence of the bulk is not yet considered. Two of them are ferroelectric ($\psi = 0$, $\phi = 0$ or π) and the third is antiferroelectric ($\psi = \pi/2$, $\phi = \pi/2$). Only the ferroelectric anchoring (FE, $\psi = 0$, $\phi = 0$) of the molecules on the surfaces can exist in the ferroelectric phase, but in the antiferroelectric phase the FE and the antiferroelectric (AF) anchoring can exist with the possibility of a transition between them induced by temperature variation.

The thermal hysteresis depicted in figure 5 can be so interpreted as follows: in the cooling curve, below 110°C (the temperature of the SmC*–SmC^*_{FI} phase transition in the bulk), the amplitude of the real part of the complex permittivity remains significant and continuously decreases up to 75°C. This can be due to the surface anchoring which can remain ferroelectric far below the antiferroelectric phase transition in the bulk. When the temperature decreases, the ratio between the antiferroelectric structure in the bulk and the FE state due to the surface anchoring increases; this leads to a continuous decrease in the real part of the complex permittivity. Close to 75°C, the surface anchoring energy can be changed from the FE to the AF state and the whole cell becomes antiferroelectric. During the heating process, upto 110°C, the bulk and the surfaces maintain the antiferroelectric structure and the AF anchoring, respectively. This state still remains several degrees above 110°C, as shown by the very weak value of the real part of the complex permittivity. In the vicinity of 117°C, the drastic increase in the real part of the complex permittivity can be associated with the antiferroelectric to ferroelectric phase transition in the bulk, and simultaneously the change from the AF to FE anchoring at the surfaces (because the AF anchoring cannot exist in the ferroelectric phase). Then, the whole cell becomes ferroelectric, inducing the drastic increase in ε' at this frequency.

5. Conclusions

A new chiral compound, with a lateral bromo substituent and exhibiting the complex dipolar, ordered smectic phases of the ferroelectric, ferrielectric and antiferroelectric kinds, has been synthesized. This material displays only one ferrielectric phase in a very narrow temperature range and the nature of this phase could not be inferred either from resonant X-ray scattering experiments [5] or from our miscibility study. Therefore

only the SmC^*_A and SmC* phases are unambiguously identified as having helix structures. The helix shows a strong twist with a change of sense between these two phases (inside the ferrielectric phase). The saturated value of the spontaneous polarization and the tilt angle in the SmC^*_A phase are about 90 nC cm^{-2} and 32°, respectively. The large thermal hysteresis, observed in the antiferroelectric phase by the dielectric measurements, has been discussed by considering two different types of anchoring (FE or AF) for the molecules on the surfaces in the antiferroelectric phase, and only one anchoring (FE) in the ferroelectric phase. The transition between the different anchoring types is induced by temperature variation. In a similar way, our study emphasizes the importance of the boundary conditions in relation to macroscopic properties measured in thin cells of antiferroelectric liquid crystals. Consequently, the assignment of the transition temperatures for the phase sequence SmC^*_A–SmC^*_{FI}–SmC*, based on the measurement of the real part of the complex permittivity, requires particular attention to thin cells.

Theoretical and experimental results concerning the importance of anchoring in relation to dielectric and electro-optic properties for thin cells containing antiferroelectric liquid crystals will be published soon.

References

[1] Clark, N., and Lagerwall, S. T., 1980, *Appl. Phys. Lett.*, **36,** 899.

[2] Chandani, A. D. L., Gorecka, E., Ouchi, Y., Takezoe, H., and Fukuda, A., 1989, *Jpn. J. appl. Phys.*, **28,** L1255.

[3] Mach, P., Pindak, R., Levelut, A. M., Barois, P., Nguyen, H. T., Huang, C. C., and Furenlid, L., 1998, *Phys. Rev. Lett.*, **81,** 1015.

[4] Mach, P., Pindak, R., Levelut, A. M., Barois, P., Nguyen, H. T., Baltes, H., Hird, M., Toyne, K., Seed, A., Goodby, J. W., Huang, C. C., and Furenlid, L., 1999, *Phys. Rev. E*, **60,** 6793.

[5] Cluzeau, P., Gisse, P., Ravaine, V., Levelut, A. M., Barois, P., Huang, C. C., Rieutord, F., and Nguyen, H. T., 2000, *Ferroelectrics*, **244,** 1.

[6] Faye, V., Rouillon, J. C., Destrade, C., and Nguyen, H. T., 1995, *Liq. Cryst.*, **19,** 47.

[7] Nguyen, H. T., Rouillon, J. C., Cluzeau, P., Sigaud, G., Destrade, C., and Isaert, N., 1994, *Liq. Cryst.*, **17,** 571.

[8] Brunet, M., and Isaert, N., 1988, *Ferroelectrics*, **84,** 25.

[9] Faye, V., Detre, L., Rouillon, J. C., Laux, V., Isaert, N., and Nguyen, H. T., 1998, *Liq. Cryst.*, **24,** 747.

[10] Miyasato, K., Abe, S., Takezoe, H., Fukuda, A., and Kuze, E., 1983, *Jpn. J. appl. Phys.*, **22,** L661.

[11] Martinot Lagarde, P., Duke, R., and Durand, G., 1981, *Mol. Cryst. liq. Cryst.*, **75,** 249.

[12] Andersson, G., Dahl, I., Keller, P., Kuczynski, W., Lagerwall, S. T., Skarp, K., and Stebler, B., 1987, *Appl. Phys. Lett.*, **51,** 640.

[13] Andersson, G., Dahl, I., Kuczynski, W., Lagerwall, S. T., Skarp, K., and Stebler, B., 1988, *Ferroelectrics*, **84,** 285.

[14] Gisse, P., Sidir, M., Lorman, V., Farhi, R., Pavel, J., and Nguyen, H. T., 1997, *J. Phys. II Fr.*, **7,** 1817.

[15] Cluzeau, P., unpublished result.

[16] Bourny, V., Pavel, J., Lorman, V., and Nguyen, H. T., 2000, *Liq. Cryst.*, **27,** 559.

[17] Hiller, S., Pikin, S., Haase, W., Goodby, J. W., and Nishiyama, I., 1994, *Jpn. J. appl. Phys.*, **33,** L1096.

[18] Gisse, P., Pavel, J., Lorman, V., and Nguyen, H. T., 1993, *Ferroelectrics*, **147,** 27.

[19] Pavel, J., Gisse, P., Nguyen, H. T., and Martinot-Lagarde, P., 1995, *J. Phys. II Fr.*, **5,** 355.